SKYLAB M553 SPHERE FORMING EXPERIMENT

By

D. J. Larson
Research Department
Grumman Aerospace Corporation
Bethpage, New York 11714

SUMMARY

The M553 Sphere Forming Experiment was conducted in the M512 Furnace Facility during Skylab II. The experiment was designed to study the effects of weightlessness in solidification processes. Four face centered cubic materials of varying alloy contents and solidification reaction types were studied.

Careful analysis of the samples indicated that there was an outstanding record of both initial and terminal solute redistribution processes, and that this record may be substantially better than that obtained terrestrially for comparable experimental conditions. Further, the last regions to solidify evidence extensive solidification terracing; and for one alloy type, this terracing was found to be decorated with second phase precipitate particles. These particles were highly localized in systematic arrays which were frequently low index crystallographic systems.

Some of the samples underwent unanticipated solidification reactions rather than the anticipated solid/liquid processes. Subsequent consideration indicated that this phenomenon could have been anticipated and that it was a result of the reduced gravity environment — that is, the reduced gravity environment magnified a typically microscopic phenomenon terrestrially so that it became a macroscopic effect. Work is continuing on quantifying this effect.

It is felt that these and subsequent results will contribute to the detailed understanding of terrestrial solidification processes and have shown the importance of considering the gas phase during space processing. Whereas prior consideration of one-gravity

solidification dealt with liquid/solid reactions, this work indicates that consideration of solid/liquid/gas reactions is important and potentially beneficial in a reduced gravity environment.

INTRODUCTION

The M553 Sphere Forming Experiment conducted in the M512 Furnace Facility during Skylab II was designed to study the effects of a reduced gravity environment on the containerless solidification of face centered cubic metals. The metals studied were: pure Ni, Ni-1 wt % Ag, Ni-12 wt % Sn, and Ni-30 wt % Cu. The constant primary crystalline structure was selected because the solidification theory for face centered cubic materials is the most advanced (Reference 1) and offered an attractive basis for planning the experimentation and evaluating the results.

The materials were electron beam melted and were either retained on stings of the same composition as the specimen or were to be released while molten, and solidified while floating free within the chamber. The latter operation was not entirely successful and some specimens intended to be released remained on their ceramic pedestals.

The present paper presents an overview of results obtained in the metallographic characterization conducted by the four investigative groups: University of Connecticut, Georgia Institute of Technology, Grumman Aerospace Corporation, and Arthur D. Little, Incorporated. We first cover features of the alloys that were similar and then features that were unique to certain alloys. In the latter area we describe a reaction that is unique to the weightless environment.

DISCUSSION

Prior to considering the differences between the different alloys, we will first discuss those features which were similar among all the alloys. It was anticipated that the reduced gravity environment would enhance the sphericity of the processed samples and this enhancement is shown in Figs. 1a and 1b for 1 g and low g specimens, respectively. Typically, the 1 g specimens had a sphericity value (R_{max}/R_{min}) of 1.28, whereas the flight samples were typically 1.01 to 1.04, a substantial enhancement due to the reduction in gravity.

Figure 2a illustrates the variation in surface morphology of both the terrestrial and flight samples. The lower portion of this sample is composed of epitaxially nucleated columnar dendrites that have grown rapidly into the melt from regions of remnant unmelted solid, or from the pedestal region. As the ratio of thermal gradient (G) to growth rate (R) decreased to a critical level, the columnar growth decayed to an equiaxed free dendritic form (Reference 2). These dendrites are located in the mid region of Fig. 2a and were the last regions to solidify. The last region to be considered is uppermost in Fig. 2a and appears to cap the other regions. This is a region of nucleation and growth that occurred on the liquid surface. The cap has assumed the dimensions of the liquid sphere, and its dimensions are thus greater than that of the lower region, which is defined by the volume of the solid. This results in the obvious height increment at the interface between the liquid surface nucleated cap and the equiaxed dendrites (Reference 3). In the cap region adjacent to the last region to solidify, there are substantial interdendritic shrinkage cavities. These are shown in Fig. 2b. The growth in the surface nucleated region progressed laterally on the two dimensional liquid surface and radially inward. The radial growth is also shown in Fig. 2b.

The relative proportion of these three regions varied depending on the thermal history of the individual samples. The samples that solidified while freely floating after total melting and those that had only a point contact of remnant unmelted solid (sting samples) solidified via surface nucleation and growth over virtually the entire sample. The samples that remained in contact with the pedestal (all of the ground base samples), that had remnant unmelted solid, or that impacted on the chamber wall during solidification all evidenced extensive areas of epitaxial growth and reduced surface nucleated growth.

An interesting aspect of the flight alloys that solidified by a surface nucleation mechanism was that all three principal growth mechanisms (platelet, cellular, and dendritic) could be active on the same surface. Microcompositional mapping in ⟨100⟩ directions indicated that the selection of growth mechanism was determined more by local thermal conditions (G, R) than by compositional fluctuation. This underscores the importance of controlling thermal parameters in containerless solidification so that the growth mechanism can be preselected.

We have introduced the areas of constancy among the samples. The differences are of equal importance and they will now be discussed.

The materials differed in solute content and in solidification reaction type. It was anticipated that the differing alloy content would affect the degree of constitutional supercooling during the bivariant portion of the solidification and would, in concert with the thermal parameters, result in a diversity of solidification mechanisms. This anticipation was confirmed: the lowest solute content alloy is (Ni-1 Ag) solidified primarily by a cellular mechanism whereas the higher solute content alloys (Ni-12 Sn, Ni-30 Cu) solidified dendritically. The sequential appearance of solidification mechanisms occurred only as surface reactions when the G/R value was sufficiently high. These flight samples reverted to the above mechanisms within the bulk of the samples as the G/R value decreased.

An additional variation was that two of the alloys (Ni-1 Ag and Ni-12 Sn) demonstrated solidification in which the bivariant solidification is superceded by a univariant solidification reaction in the last regions to solidify. These reactions were, respectively, monotectic and eutectic in nature. These univariant reactions gave some interesting results.

Considering the eutectic solidification of the Ni-12 Sn alloy first, the proeutectic solidification in the last regions to solidify was dendritic. The interesting features were that the proeutectic dendrite tips were clearly terraced where they were exposed by interdendritic solidification shrinkage, and that some of those dendrites were decorated by arrays of the intermetallic (Ni_3Sn) eutectic constituent. Careful investigation of the platelet and cellular solidification regions of the flight samples indicated terracing during these mechanisms, as well, although they were not decorated with intermetallic particles. The platelet and dendritic terracing is shown in Figs. 3a and 3b, respectively. The highly localized decoration of the dendrite tips is shown in Fig. 4a and 4b. These latter results were not typical of the particle decoration found in the ground base samples and may be a manifestation of reduced convection level in the flight samples. Terracing, too, was substantially less marked and may have been enhanced by reduced convection.

The last feature to be discussed relates primarily to the Ni-1 Ag samples, but was noted to a lesser extent in some of the

Ni-12 Sn flight samples. These features were internal voids that formed during the processing. Their volume was such that they could not have resulted from solidification shrinkage. They actually caused distortions of the outer surfaces. This can be seen in Figs. 5a and 5b for Skylab Samples 1.2 and 1.13, respectively.

Transverse sections of the voids are shown in Figs. 6a and 6b for the Ni-1 Ag and Ni-12 Sn, respectively. Careful microchemical analysis of the inner surfaces of the voids indicated that they were not a result of interstitial contaminant gas, but were due to metallic gas evolution during the processing (Reference 3). This revealed some interesting internal artifacts of both melting and solidification, as shown respectively in Figs. 7a and 7b. In the former case (Fig. 7a) the microchemical banding of the starting material has resulted in preferential melting of solute rich regions in advance of the solute poor regions. The subsequent volatilization of the silver rich liquid has laid bare the melting interface of this partially melted sample. In the latter case, the advancing solidification interface has also been revealed because of volatilization of the solute enriched liquid. Whereas these results are intriguing and potentially useful as a technique for revealing melting or solidification interfaces, the question arises as to why these reactions occurred to a much greater extent in the Ni-1 Ag flight samples than in the ground base samples, and why they occurred in the Ni-12 Sn flight samples when they had not been noted in the ground base samples. Consideration of this anomaly led us to a rigorous review of the processing parameters and to how these parameters would affect the solidification reactions. In turn, this led us to consider pressure (P) - temperature (T) - composition (X) diagrams for the alloys in question, rather than the conventional temperature (T) - composition (X) diagrams, because the T-X phase diagrams were generated under 1 g and one atmosphere of pressure, whereas the experimental conditions during the flight were 10^{-3} g and 10^{-5} mm of Hg. Consideration of reduced pressure isobaric sections within both P-T-X diagrams indicated that metallic gas evolution could occur as a phase reaction within both systems, on cooling (Reference 3). The reason that the reduced pressure reaction was suppressed within the ground base samples was due to the hydrostatic pressure head within the liquid itself. The hydrostatic pressure head is given by Eq. (1) for a cylindrical column of liquid

$$\Delta P = \omega h = \rho g h \qquad (1)$$

where ΔP = pressure increment, ω = specific weight, h = distance from the surface into the liquid, ρ = density, and g = gravity. It is clear that the pressure head decreases with reduction in gravity, and the prescribed low pressure phase reactions may become bulk reactions rather than surface reactions. This substantially broadens the consideration of space processing from liquid/solid phenomena to liquid/solid/gas phenomena and emphasizes that the pressure of a reduced gravity environment might prove to be a significant consideration for future experimentation. This point is being actively pursued.

CONCLUSIONS

In conclusion, we might say that this space experiment confirmed many results that had been anticipated, but in several important respects the results were unanticipated. The record of terracing was excellent, although not unprecedented terrestrially. The highly localized precipitate arrays, however, are more unusual and these results should be considered in light of existing theory of solute redistribution. Further, an additional process has been demonstrated that can address the problem of revealing the solid/liquid interface. Lastly, the importance of a rigorous consideration of the process parameters during space processing has been demonstrated. Although thermal control has previously been considered important, pressure control may prove to be an important consideration as well.

We have demonstrated that the pressure head is directly (and in a manner that may be quantified) related to gravity, and that as a result of the reduction of this head low pressure phase reactions may occur in the bulk that could not occur otherwise. Applications of these phase reactions are only limited by the creativity of the experimentalist, and it should be pointed out that these reactions are sufficiently rare terrestrially as to be unnamed.

ACKNOWLEDGMENTS

This work was partially supported by NASA Contract NAS 8-28728. We would also like to acknowledge the support of Mr. Earl Hasemeyer (who was the COR on this program) and Mr. Charles Lovoy, both of NASA, Marshall Space Flight Center.

REFERENCES

1. Tiller, W. A., J. Metals, Vol. 9, p. 847, 1957.

2. Kattamis, T. Z., "Phase C. Report - Evaluation of Skylab Samples," Institute of Materials Science, the University of Connecticut, December 1973.

3. Larson Jr., D. J., "Final Report on Phase C - Specimen Analysis of Skylab, M553 Experiment, Flight Samples," Research Department, Grumman Aerospace Corporation, April 1974.

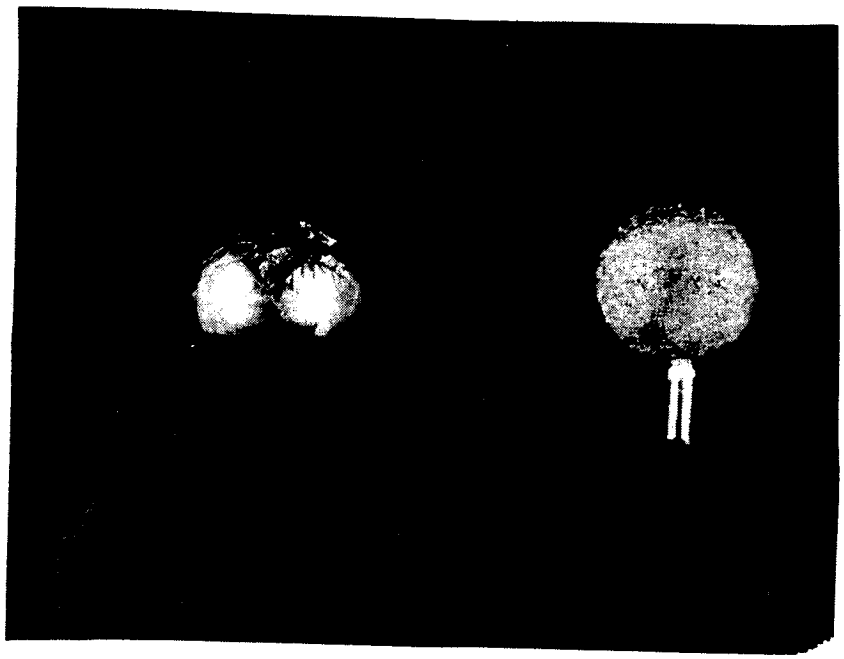

(a) (b)

FIGURE 1. MACROPHOTOGRAPHS OF 1 g PROCESSED AND LOW g PROCESSED SPHERES (2X)

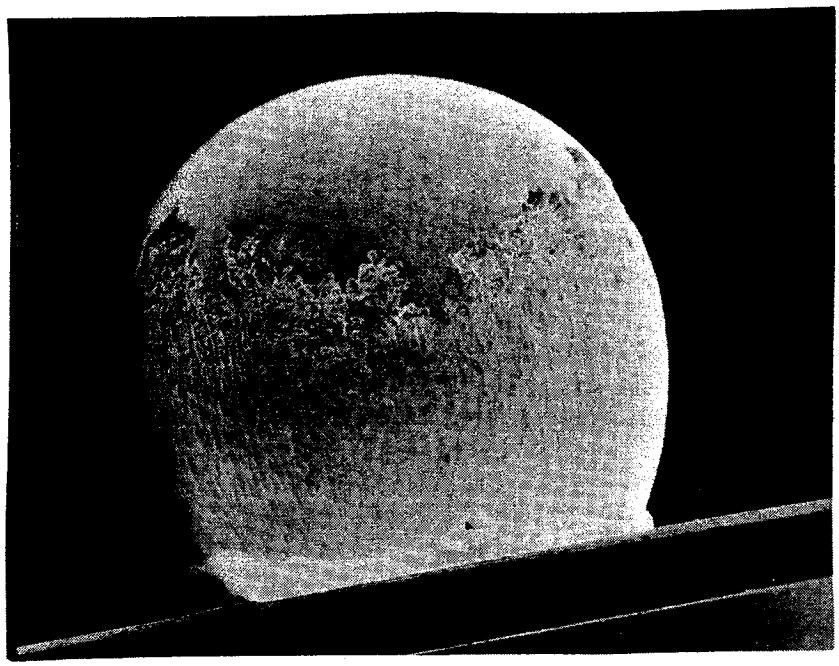

FIGURE 2A. MACROPHOTOGRAPH OF Ni-30 Cu SKYLAB SAMPLE 1.7 SHOWING REGIONS OF VARYING GROWTH MORPHOLOGY (15X)

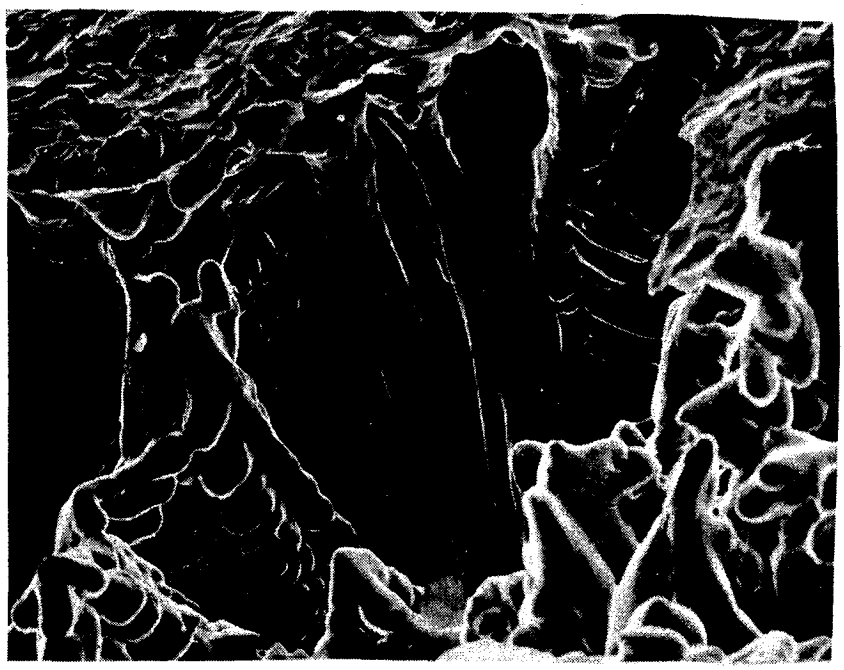

FIGURE 2B. ENLARGEMENT OF INTERFACE REGION OF THE Ni-30 Cu SKYLAB SAMPLE 1.7 SHOWING RADIAL GROWTH INWARD OF THE SURFACE NUCLEATED GRAINS (400X)

FIGURE 3A. TERRACING AT THE EXTREMITIES OF THE PLATELET GROWTH IN Ni-12 Sn SKYLAB SAMPLE 2.3 (3750X)

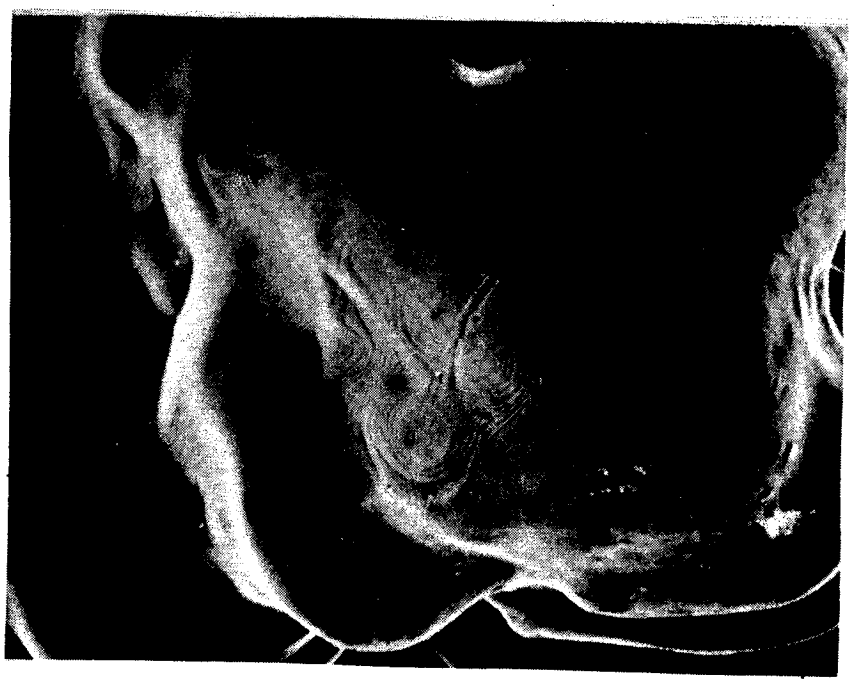

FIGURE 3B. TERRACING ON PRIMARY AND SECONDARY DENDRITE ARMS IN Ni-12 Sn SKYLAB SAMPLE 2.3 (3750X)

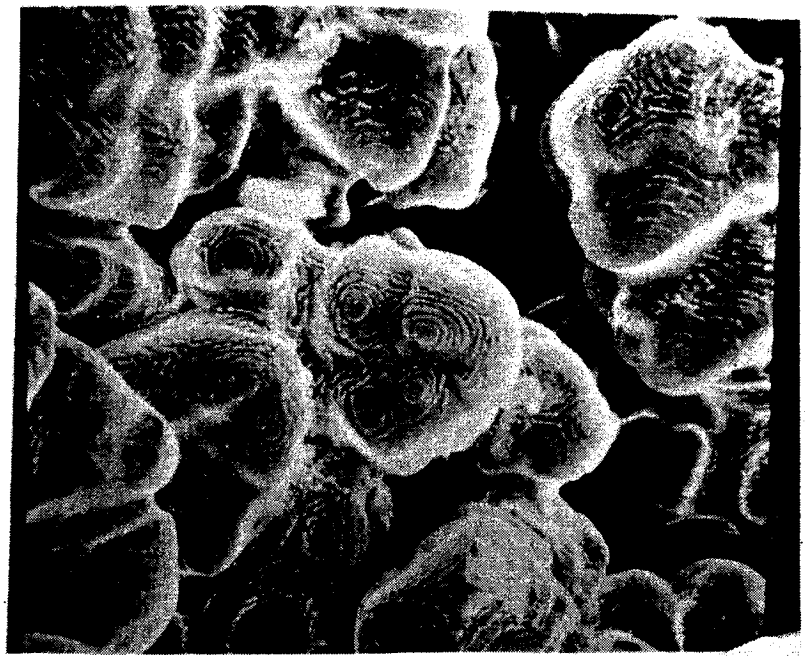

FIGURE 4a. DECORATION OF TERRACES BY Ni_3Sn EUTECTIC CONSTITUENT IN Ni-12 Sn SKYLAB SAMPLE 1.6 (1000X)

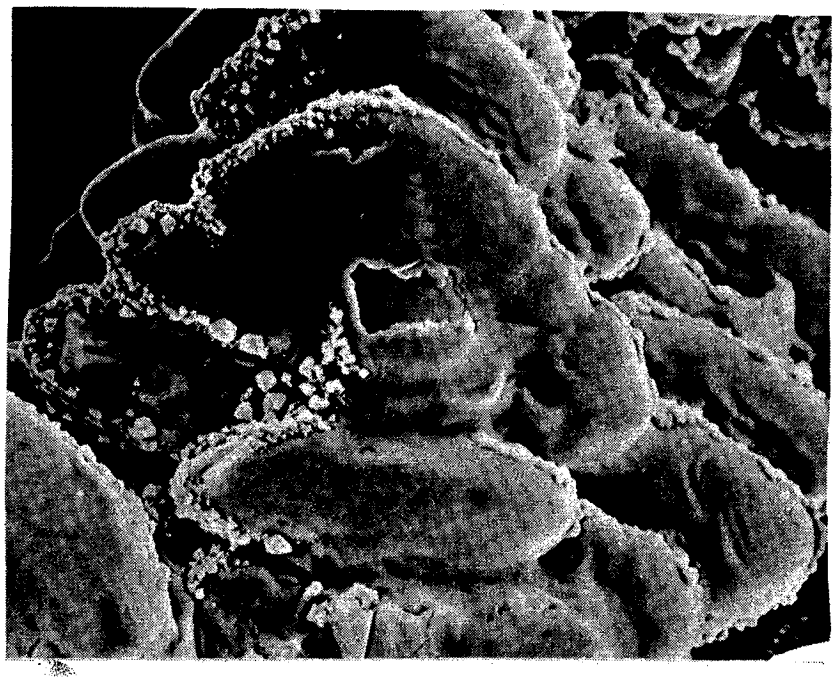

FIGURE 4b. DECORATION OF Ni_3Sn PARTICLES IN A CRYSTALLOGRAPHICALLY DEFINED ARRAY Ni-12Sn SKYLAB SAMPLE 2.3 (1500X)

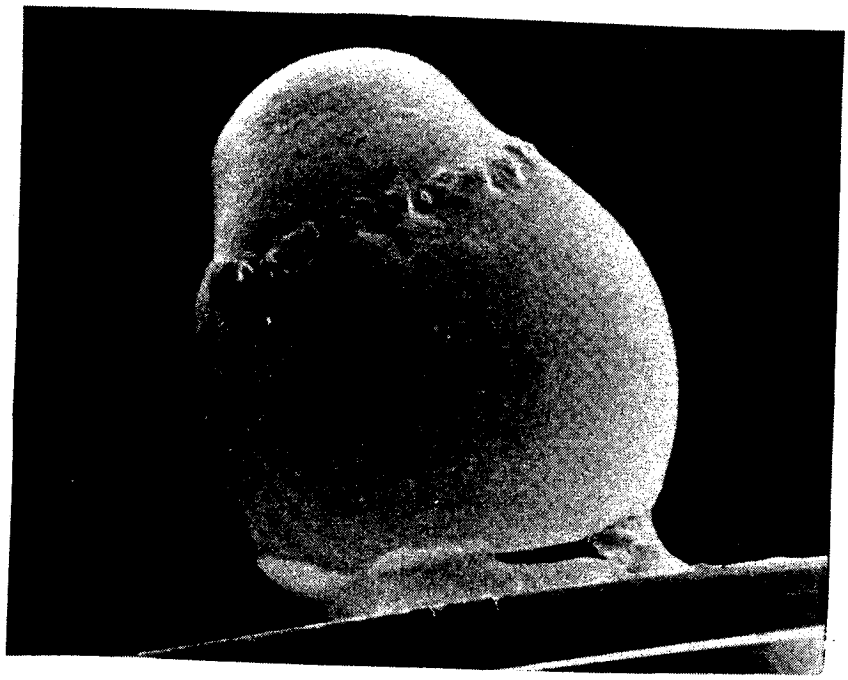

FIGURE 5a. MACROSCOPIC DISTORTION OF Ni-1 Ag
SKYLAB SAMPLE 1.2 (15X)

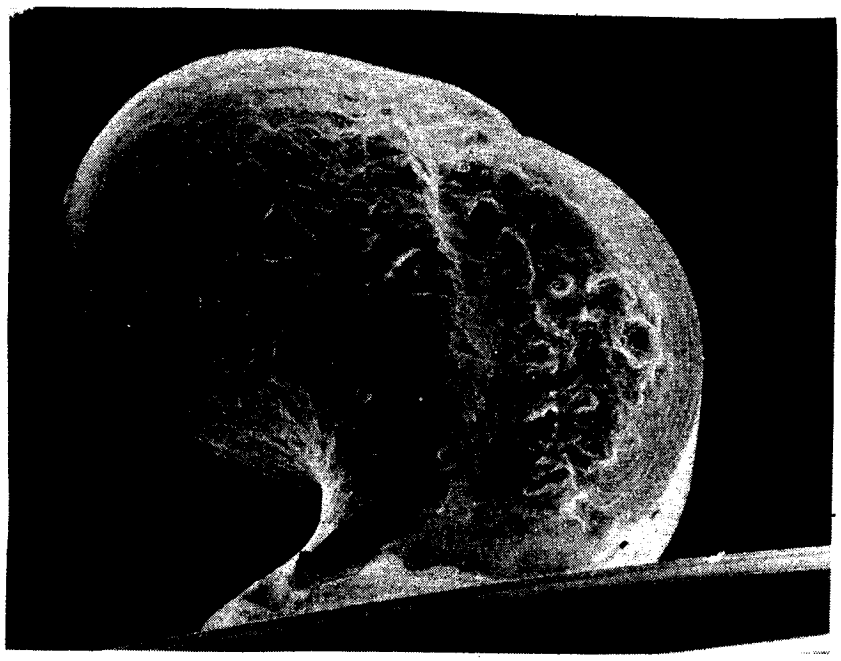

FIGURE 5b. MACROSCOPIC DISTORTION OF Ni-1 Ag
SKYLAB SAMPLE 1.13 (15X)

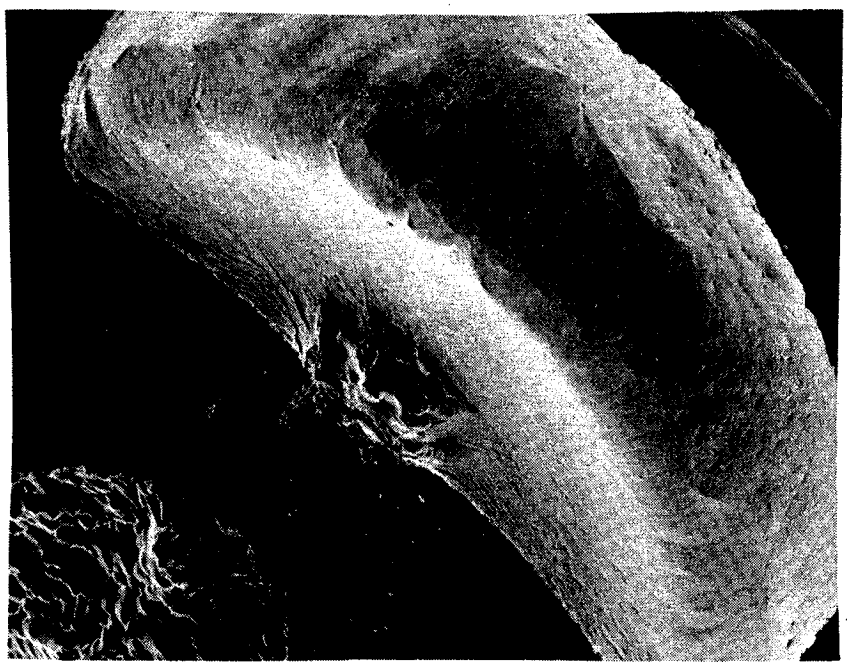

FIGURE 6a. MACROSCOPIC VIEW OF VOID AREAS IN Ni-1 Ag SKYLAB SAMPLE 1.2 (35X)

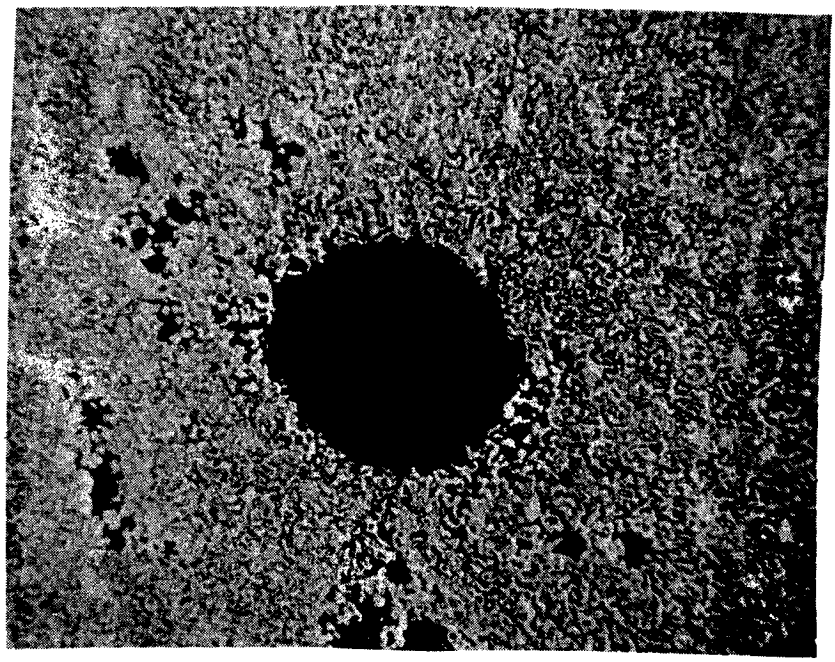

FIGURE 6b. MACROSCOPIC VIEW OF VOID AREA IN Ni-12 Sn SKYLAB SAMPLE 2.7 (60X)

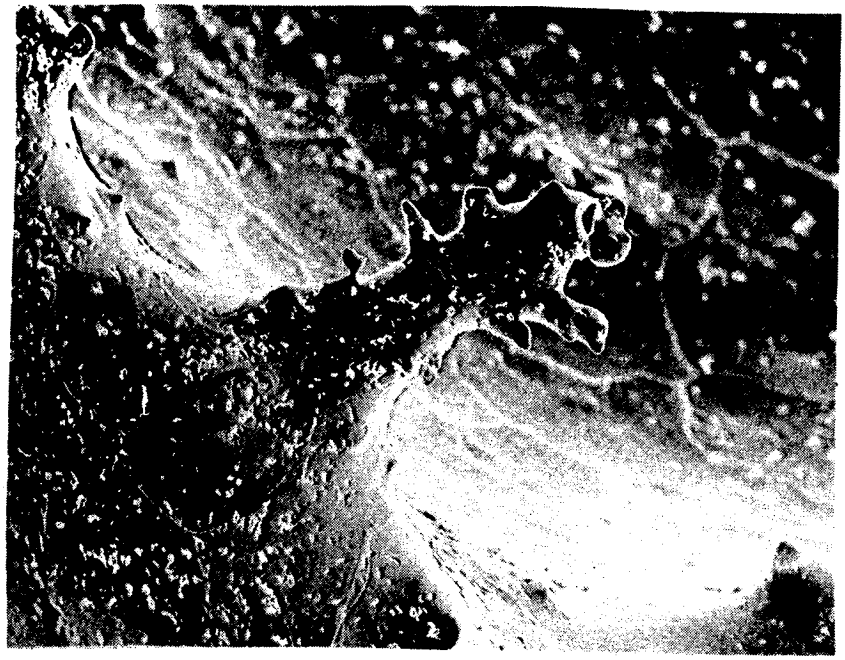

FIGURE 7a. MICROPHOTOGRAPH OF MELTING ARTIFACT REVEALED BY LIQUID/SOLID/GAS REACTION IN Ni-1 Ag SKYLAB SAMPLE 1.13 (400X)

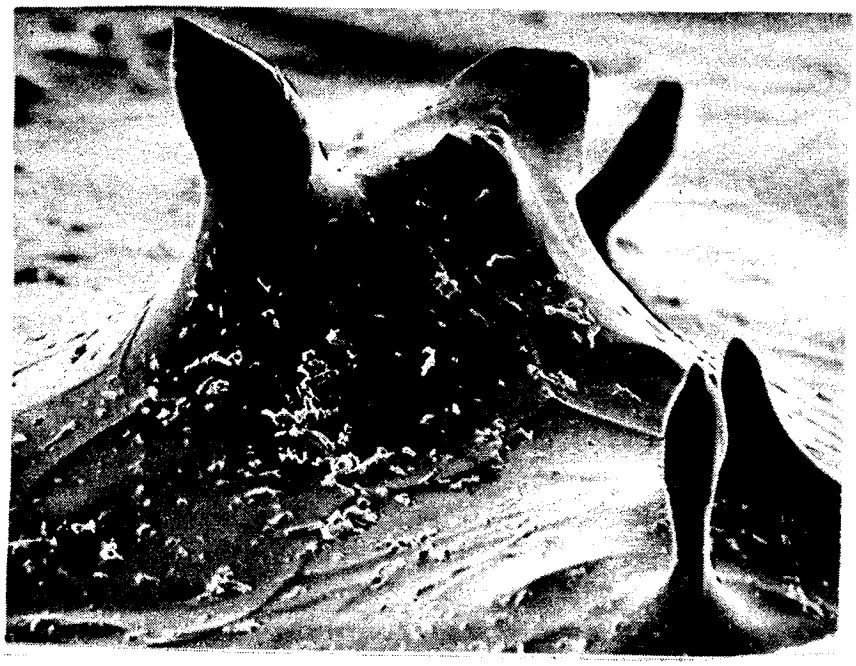

FIGURE 7b. SOLIDIFICATION ARTIFACT REVEALED BY LIQUID/SOLID/GAS REACTION IN Ni-1 Ag SKYLAB SAMPLE 1.13 (1500X)